ACS APPLIED POLYMER MATERIALS

pubs.acs.org/acsapm

Article

Starch Films Plasticized by Imidazolium-Based Ionic Liquids: Effect of Mono- and Dicationic Structures and Different Anions

Susanna Romano, Serena De Santis, Andrea Martinelli, Lorenzo Augusto Rocchi, Daniele Rocco, Giovanni Sotgiu, and Monica Orsini*

Cite This: ACS Appl. Polym. Mater. 2023, 5, 8859−8868

Read Online

ACCESS | Metrics & More | Article Recommendations | Supporting Information

ABSTRACT: Recently, imidazole-based ionic liquids have been widely used as starch plasticizers. These salts are very effective in transforming starch, a widely available and inexpensive biopolymer, into biodegradable films with good mechanical properties and ionic conductivity. These films could have interesting applications in flexible electronics and solid polymer electrolytes. Since a wide variety of cation−anion combinations can be used, it is useful to evaluate the impact of different anion and cation structures on the properties of plasticized starch to select the most suitable ionic liquid for each specific application. In this work, starch films plasticized with imidazolium-based ionic liquids were prepared by the solution casting method. 1-Ethyl-3-methyl imidazolium was chosen as a cation and the effect of different anions such as $[SO_4Et]^-$, $[N(CN)_2]^-$, $[OAc]^-$, and $[Cl]^-$ on the film properties was investigated. In addition, a dicationic structure, consisting of two closely bonded imidazolium rings, was also considered. The characteristics of the corresponding starch-based films were analyzed and compared with those of films prepared with monocationic ionic liquids.

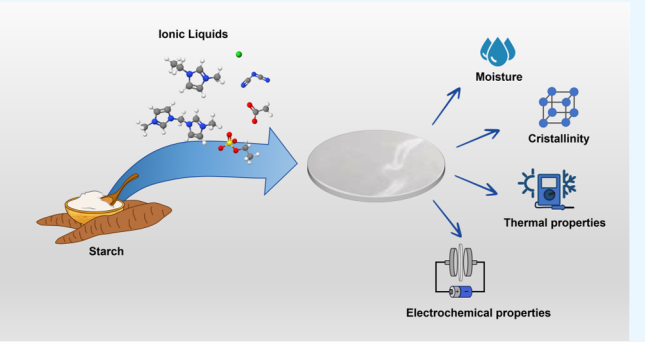

KEYWORDS: *thermoplastic starch, ionic liquid plasticizers, mono/dicationic imidazolium structure, anion effect, conductive films*

1. INTRODUCTION

Petroleum-derived plastics are commonly used for many applications because they can be easily tailored according to the product requirement due to their formidable features. However, if not properly recycled, these non-biodegradable materials, are responsible for high environmental pollution.[1] The progressive replacement of conventional plastics with bioplastics derived from non-oil macromolecules, which are biodegraded in shorter times, is a great challenge.[2]

Bioplastics can be obtained from natural polymers such as polysaccharides, proteins, and lipids or generated by microorganisms in fermentative processes using an appropriate carbon source.[3] Among biopolymers, starch is one of the most promising to replace petroleum-based plastics[4,5] since it is completely biodegradable, inexpensive, and widely accessible in plants such as corn, cassava, potato, tuber, and others. Native starch exists in the form of granules, which are composed of amylose and amylopectin. The shape of the granules and the percentage of amylose and amylopectin depend on the botanical sources from which starch is derived. Amylose is a linear polysaccharide based on $\alpha(1-4)$ bonds, while amylopectin is a highly branched carbohydrate whose units are linked by $\alpha(1-4)$ and $\alpha(1-6)$ bonds, which are responsible for the branching points that occur every 22−70 units of glucose.[6]

The granules show a complex organized structure with alternating concentric amorphous and semicrystalline regions. Amylose and branching connection of amylopectin produce amorphous zones, while the short chains in the amylopectin compose the crystalline fraction.[7] The semicrystalline nature of starch and the ability of each unit to form strong inter- and intramolecular hydrogen bonds,[8] need to be altered to obtain a material with the performance characteristics of conventional plastics.[9]

Various physical or chemical modifications, such as plasticization, blending, derivation, and graft copolymerization, have been proposed.[10−12] Plasticizers have been widely used in the modification of polymers since the early 1800s. By a heating treatment and the addition of a plasticizer, the 3D structure of native starch can be destroyed, and thermoplastic starch is obtained to produce starch-based bioplastics. Polyols, such as glycerol and sorbitol,[13,14] or other compounds[15] including urea[16] and citric acid,[17] are the most studied and

Received: June 9, 2023
Revised: October 12, 2023
Accepted: October 12, 2023
Published: November 1, 2023

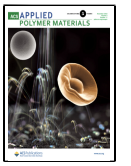

used plasticizers. However, small molecules are likely to diffuse out from polymeric materials after a short time, causing changes in the material properties.[18]

Ionic liquids (ILs) have attracted much interest in the past few years in the academy and industry due to their enormous potential as substitutes for traditional plasticizers. Ionic liquids are salts in liquid state below 100 °C.[19] Being entirely composed of ions, they possess negligible vapor pressure and are non-flammable. A very interesting feature of ionic liquids is the possibility of obtaining different cation and anion combinations, which are estimated to equate to a million ILs.[20] This allows their intrinsic characteristics, such as conductivity, density, viscosity, melting point, and polarity, to be finely tuned.[21]

Imidazolium-based ionic liquids have extensively been studied for a variety of applications and have recently been used to plasticize starch films.[20] The use of these salts made it possible to transform starch into a material with good plastic properties and to produce starch-based ion-conducting polymers[22] or solid polymer electrolytes.[23] Many different types of monocationic imidazolium-based ionic liquids have been tested, producing starch-based bioplastics with good characteristics.[20] Given the large number of combinations of different anions and cations, it is of great interest to determine the effect of their chemical structures on the properties of starch-based materials. This understanding will make it possible to select an appropriate combination of cations and anions to produce biopolymers with the required properties.

In this work, 1-ethyl-3-methyl imidazolium-based ionic liquids with different anions were used as plasticizers to prepare starch films by a solution casting technique. The influence of different anions ($[SO_4Et]^-$, $[N(CN)_2]^-$, $[OAc]^-$, and $[Cl]^-$) on the morphology, crystalline structure, glass transition temperature, thermal stability, and electrical conductivity of the films were investigated.

To gain further insight into the role of the IL structure, a salt composed of a chloride anion and two 1-ethyl-3-methyl imidazolium-based cations linked with a short spacer was synthesized.[24] This investigation can provide useful insights into the use of this class of ionic liquids[25−27] to prepare starch-based plastic materials.

2. EXPERIMENTAL SECTION

2.1. Materials. Arrowroot starch (16−27% content of amylose[28]), 1-methylimidazole (Alfa Aesar), dichloromethane (CH_2Cl_2, Sigma-Aldrich), dimethyl sulfoxide (DMSO, Sigma-Aldrich), diethyl ether (Sigma-Aldrich), 1-ethyl-3-methyl imidazolium ethyl sulfate (EMIm-SO_4Et), 1-ethyl-3-methyl imidazolium dicyanamide (EMIm-N-$(CN)_2$), 1-ethyl-3-methyl imidazolium chloride (EMIm-Cl, Sigma-Aldrich), and 1-ethyl-3-methyl imidazolium acetate (EMIm-OAc, Sigma-Aldrich) were used as received.

2.2. Synthesis of 3,3′-Methylenebis(1-methyl-1*H*-imidazol-3-ium) Dichloride. The preparation of the dicationic ionic liquid ($C_1(MIm)_2\ Cl_2$) was performed with little changes from the method described by Penn et al.[29] In a round-bottom flask with 1.15 mL of DMSO, 1-methylimidazole (20 mmol) and CH_2Cl_2 (60 mmol) were added together. The reaction was conducted under stirring at 100 °C for 24 h. The resulting white insoluble precipitate was washed three times with diethyl ether to remove the DMSO and any trace of unreacted imidazole. The product (0.4 g) was dried in rotavapor without the need for further purification. ^{1}H NMR and ^{13}C NMR (Bruker AVANCE-400 spectrometer) spectra were used to confirm the structure of synthesized 3,3′-methylenebis(1-methyl-1*H*-imidazol-3-ium) dichloride (spectra are provided in Supporting Information Figures S1 and S2).

2.3. Preparation of Starch Films. Starch films were prepared by the solvent casting and evaporation method. First, an amount of 1 g of arrowroot starch was dissolved in 30 mL of distilled water for 30 min with stirring until completely gelatinized at 95 °C. Although a specific gelatinization temperature range exists for each type of starch, there is a general consensus in the literature that above 90−95 °C gelatinization can be considered complete.[30] Then, an amount of 0.4 g of plasticizer (EMIm-X or $C_1(MIm)_2\ Cl_2$)[31] was added to the solution and heated for 10 min at the same temperature until the mixture was homogeneous. The solution was then cooled to 65 °C and poured into a silicone Petri dish (diameter: 90 mm), dried for 24 h in an oven at 45 °C, and finally left for 24 h at room temperature. Dried films were peeled off from the casting plate and maintained at 50% relative humidity (RH).

2.4. Film Characterizations. *2.4.1. Film Thickness.* The thickness of the films was determined by a digital caliber, making three measurements on three distinct points for each film.

2.4.2. Scanning Electron Microscopy. A scanning electron microscope (SEM, Coxem CX-200 Plus SEM, South Korea) was employed to examine the morphology of the films at 13−15 kV acceleration voltage and 5 nm spot size. For all the images, a magnification of 1000× was used. The film samples were mounted on aluminum stubs and fixed by double-sided adhesive tape. Subsequently, the samples were coated with a thin golden layer (0.01−0.1 μm) to prevent charging.

2.4.3. Moisture Content. The moisture content (MC) of the films conditioned at 50% relative humidity was calculated gravimetrically by using the following equation

$$\text{moisturecontent}(\%) = \frac{(M_i - M_f)}{M_i} \times 100 \quad (1)$$

where M_i and M_f are the weights of the sample before and after drying at 105 °C for 24 h.

2.4.4. X-ray Diffraction Analysis (XRD). XRD analyses were performed on film samples (stored at room temperature at 50% RH) at ambient conditions by an XRD apparatus (Smartlab SE, Rigaku Corporation, Tokyo, Japan) with a Cu Kα radiation source (λ = 1.54 Å) at 40 kV voltage and 50 mA current. Intensities were collected by step scanning in the 5−40° (2θ) range, with a step of 0.01° and a scan speed of 1.50° min^{-1}. Equation 2 was used to estimate the crystallinity of different samples[32]

$$\chi_c = \frac{\sum_{i=1}^{n} A_{ci}}{A_t} \quad (2)$$

where A_{ci} is the area under each crystalline peak and A_t is the total area, both amorphous and crystalline, under the diffractogram.

2.4.5. Fourier Transform Infrared Spectroscopy (FTIR). The FTIR spectra in the 4000−650 cm^{-1} region were collected using a Nicolet iN10 infrared microscope (Thermo Fisher Scientific IT, Milano, Italy) equipped with a mercury−cadmium−telluride (MCT-A) nitrogen-cooled detector in the ATR mode. Sixty-four interferograms were averaged per spectrum and apodized using a Blackman−Harris correction. The background spectrum was collected on air. The nominal spectral resolution was 8 cm^{-1}. Data acquisition and spectra elaboration were carried out with OMNIC SPECTA software provided by Thermo Fisher Scientific.

2.4.6. Thermogravimetric Analysis (TGA). The thermal stability of starch films was evaluated by thermogravimetric analysis (TGA) by employing a Mettler TG 50 thermobalance. A thermal scanning interval of 25−500 °C and a scanning speed of 10 °C/min were set. Analyses were carried out under a nitrogen flow on a 5−6 mg sample weight. The degradation temperature was determined in correspondence with the peak of the first derivative of the weight with respect to temperature.

2.4.7. Differential Scanning Calorimetry (DSC). Thermal properties of the cast films (conditioned at RH of 50%) were evaluated by differential scanning calorimetry (Mettler Toledo DSC 822e). All of the analyses were carried out under a nitrogen flow (30 mL min^{-1}) on

https://doi.org/10.1021/acsapm.3c01235
ACS Appl. Polym. Mater. 2023, 5, 8859−8868

about 4−8 mg of sample. The glass transition temperature was defined as the midpoint of the heat capacity increase.

The applied temperature program is as follows: first, the samples were placed on sealed capsules and cooled to −50 °C. Then, a temperature ramp up to 100 °C at 10 °C min^{-1} was applied without detecting water crystallization or fusion peaks. The second series of experiments was carried out on opened capsules to dry the samples: they were first heated from 20 up to 150 °C, then cooled to 20 °C, and heated again up to 200 °C at 10 °C min^{-1}. The glass transition temperatures were reported as dry T_g.[21]

2.4.8. Mechanical Tests. Mechanical features, namely, tensile strength (TS), Young's modulus (E), and elongation at break (ε%) of films were determined by tensile tests by using an ISTRON 4502 instrument (Instron Inc., Norwood, MA, USA). For the analysis, the films (stored at room temperature at 50% RH) were cut into rectangular specimens (63.5 mm × 9.53 mm × (0.120−0.200) mm) and fixed between the two flat jaw grips. Measurements were carried out at a 10 mm min^{-1} deformation rate with a 2 kN load cell.

2.4.9. Electrochemical Properties. Ionic conductivity measurements were carried out on a polymer film sandwiched between two blocking stainless steel metal electrodes with a total surface area of 0.95 cm^2 by using electrochemical impedance spectroscopy. The measurements were performed by Metrohm Autolab PGSTAT204 with an ac amplitude of ±10 mV over a frequency range of 1 MHz to 1 Hz. The conductivity of starch films was tested at room temperature under controlled humidity (RH = 50% and RH = 40%), during a temperature scan. The conductivity was calculated using eq 3, where l is the film thickness, A is the film area, and R (Ω) is the film resistance derived from the intercept of the Nyquist plot (Z' vs Z'') with the real axis

$$\sigma(\mathrm{S/cm}) = \frac{l}{A \times R} \quad (3)$$

The working electrochemical window of the samples was measured by using the linear sweep voltammetry (LSV) technique. The voltage applied increases from 0 to 3 V with the scan rate of 1 mV s^{-1}.

3. RESULTS AND DISCUSSION

3.1. Preparation of Starch Films. Starch-based films were prepared using a solution casting technique employing 40 wt % of plasticizer with respect to the dry starch to ensure a good plasticizing effect, as reported in the literature.[33,34]

Four ionic liquids with 1-ethyl-3-methyl imidazolium $[EMIm]^+$ as cation and different anions, namely, $[SO_4Et]^-$, $[N(CN)_2]^-$, $[OAc]^-$, and $[Cl]^-$, were selected as plasticizers (Figure 1a). These specific ions were chosen based on their different size and charge distributions to investigate their different ability to plasticize starch and produce conductive films. In addition, to examine the impact of a doubly charged cation, the symmetrical dicationic ionic liquid 3,3′-methylenebis(1-methyl-1*H*-imidazol-3-ium) dichloride ($C_1(MIm)_2Cl_2$) was synthesized and used to plasticize the starch (Figure 1b). All obtained films were characterized to evaluate their physical−chemical properties based on the ionic liquid used.

3.2. Appearance, Morphology, and Water Content. All prepared films showed a homogeneous surface without bubbles. They exhibited a brilliant face in contact with the silicone dish and a matt surface exposed to air during drying, as also observed in a previous study.[35] The thickness of the prepared films ranged from 0.14 to 0.16 mm for all of the samples, except for TPS_EMIm-$N(CN)_2$, which showed a thickness of around 0.18 mm.

Table 1 reports the moisture content of each film. The TPS_EMIm-SO_4Et and TPS_EMIm-$N(CN)_2$ show the lowest water content compared to other films. Probably, the higher hydrophobicity of these two plasticizers can affect the film's ability to retain water.[36,37]

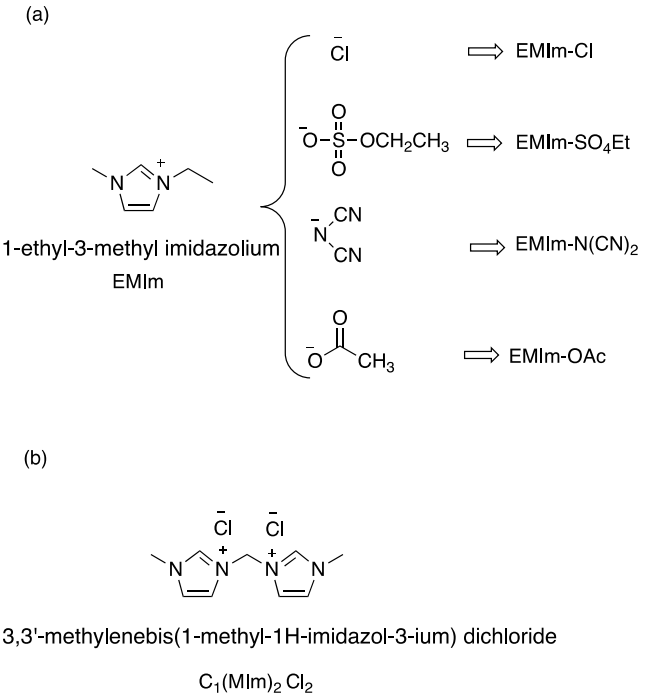

Figure 1. (a) Monocationic and (b) dicationic ionic liquids used as plasticizers.

Table 1. Moisture Content (MC) of the TPS Samples

sample	moisture content (%)
TPS_EMIm-SO_4Et	8 ± 1
TPS_EMIm-OAc	19 ± 1
TPS_EMIm-$N(CN)_2$	9 ± 1
TPS_EMIm-Cl	14 ± 1
TPS_$C_1(MIm)_2$ Cl_2	12 ± 1

All starch films displayed good transparency (as an example, the images of TPS_EMIm-Cl and TPS_$C_1(MIm)_2$ Cl_2 are reported in Figure S3), showing the proper plasticization of starch by the ionic liquids used.[38] The morphologies of the different starch samples were determined by scanning electron microscopy (Figure 2). All of the plasticized films (Figure 2A−E) showed a homogeneous surface without evident remnant structures, demonstrating the ability of such plasticizers to satisfactorily disrupt starch granules during the gelatinization process.[32]

Regarding the film obtained using ionic liquid EMIm-SO_4Et (Figure 2A), a slightly rougher surface can be seen, probably due to less interaction between the starch and the plasticizer.

3.3. X-ray Diffraction Analysis (XRD). The crystallinity of the starch film samples was analyzed by the X-ray diffraction (XRD) technique. Previous studies[39,40] have shown that in the native starch, amylopectin can exist in two possible polymorphic structures called A-type and B-type, showing distinguishing XRD patterns.[41] After processing and addition of guest molecules as plasticizers, the amylose, which is not crystalline in the native state, can be transformed into a V_H-type structure.[42] The various crystal structures of starch interact differently with the water molecules. In detail, the A-type structure has a monoclinic unit structure that contains two double helices and four water molecules. Instead, the B-

https://doi.org/10.1021/acsapm.3c01235
ACS Appl. Polym. Mater. 2023, 5, 8859−8868

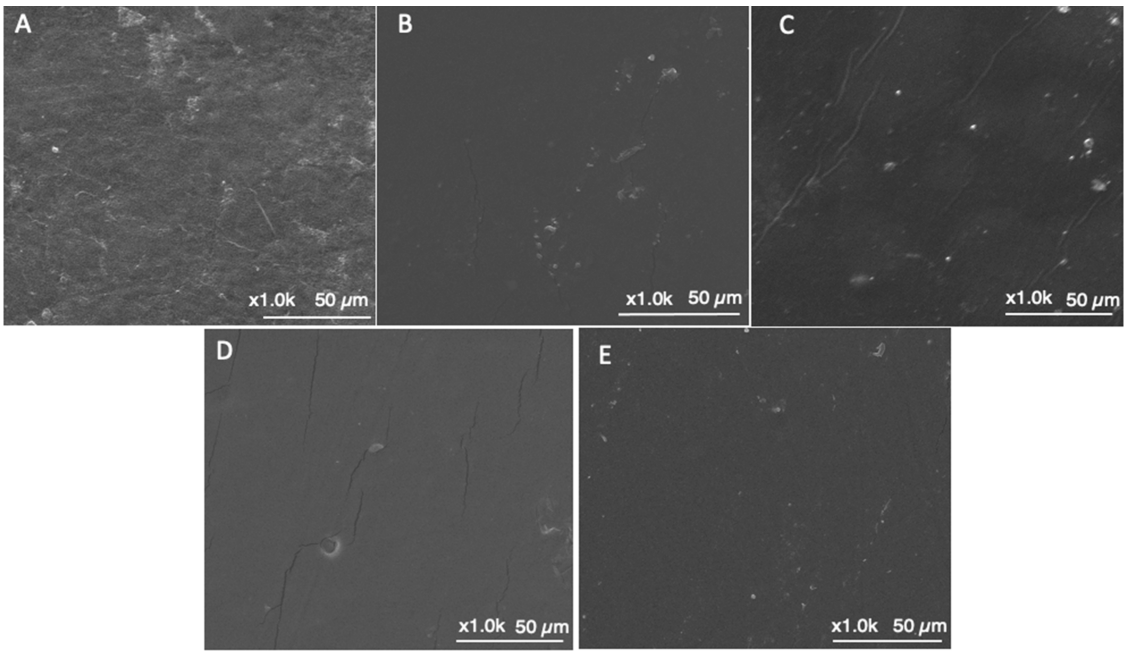

Figure 2. Scanning electron microscopy images of surface morphologies of (A) TPS_EMIm-SO_4Et, (B) TPS_EMIm-$N(CN)_2$, (C) TPS_EMIm-OAc, (D) TPS_EMIm-Cl, and (E) TPS_$C_1(MIm)_2$ Cl_2.

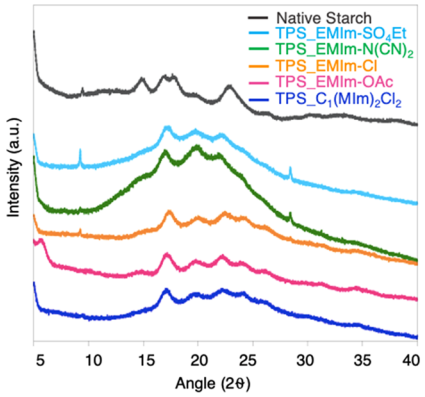

Sample	χ_c(%)			
	Total	A-type	B-type	V_H-type
Native starch	78	61	-	17
TPS_EMIm-SO_4Et	39	-	14	25
TPS_EMIm-OAc	39	-	25	14
TPS_EMIm-$N(CN)_2$	41	-	14	27
TPS_EMIm-Cl	38	-	23	15
TPS_ $C_1(MIm)_2$ Cl_2	45	-	28	17

Figure 3. XRD patterns and parameters for the crystalline structure of native starch and TPS films.

type is organized as a hexagonal unit with two double helices and 36 water molecules. Lastly, the V_H-type structure is organized in single helices, which have hydrophilic outer surfaces and a hydrophobic central cavity.[42]

In this work, the spectrum of native starch showed the typical A-type pattern with strong diffraction peaks at 15 and 23° and the characteristic doublet at 2θ of 17 and 18° (Figure 3). This pattern also showed weak peaks at 26°, 30°, and 33°. In the plasticized samples, the doublet disappeared, the peak at 15° became very weak, suggesting a loss in A-type content and the intensity of the peak at 20° increased, indicating an increase of the V_H-type structure. In addition, all starch samples displayed a peak at 2θ of around 17° and a few smaller peaks at 22° and 24°, which were characteristic of the B-crystalline structure. Although starch samples plasticized with different ionic liquids formed V_H-type and B-type crystal structures, the crystallinity was found to be lower than that of native starch, as indicated by the reduced XRD intensities whose values are reported in Figure 3.

It can be observed that the TSP_EMIm-$N(CN)_2$ and TSP_EMIm-SO_4Et samples showed a higher contribution of V_H-type (the peak at 20° is more evident) compared to the TSP_EMIm-Cl and TSP_EMIm-OAc ones in which the B-type structure appears to be prevalent (the intensity of the peak at 20° decreases, and the peaks at 22 and 24° are more prominent). The B-type structure can be associated with a higher amount of retained water in accordance with the moisture content observed in the film with EMIm-Cl and EMIm-OAc (Table 1). As confirmation, a peak at 2$\theta \approx 5°$ appeared in the spectrum of the sample plasticized with EMIm-OAc, typical of the B-type structure when the specimen has a high level of hydration.[42] The XRD parameters reported in Figure 3, related to the crystalline structure, confirmed the considerations reported above.

When the dicationic ionic liquid $C_1(MIm)_2Cl_2$ was used as a plasticizer, the crystallinity of the film, although lower than that of native starch, was higher than those of the films plasticized with monocationic ionic liquids (Figure 3). The XRD spectrum of this film was very similar to that of the starch sample plasticized with the monocationic counterpart EMIm-Cl (Figure 3). Indeed, the starch structure in this film appeared to be predominantly B-type. Therefore, it can be assumed that

https://doi.org/10.1021/acsapm.3c01235
ACS Appl. Polym. Mater. 2023, 5, 8859−8868

in the reorganization of the starch structure after processing, the anion is involved much more than the cation.

3.4. FTIR Analysis. FTIR analyses were performed to study the interaction between the plasticizers and starch. The spectra of the samples are reported in Figure 4. The spectrum of the

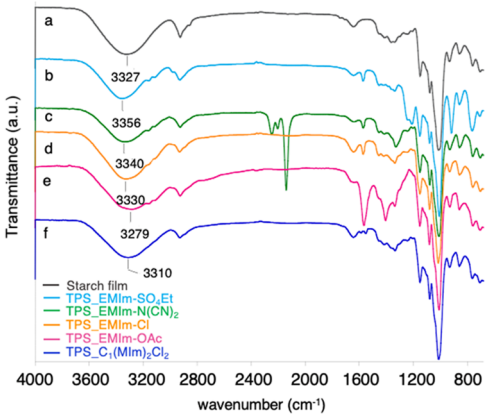

Figure 4. FTIR spectra of the TPS samples.

starch film without ILs (Figure 4a) showed absorption bands associated with C−O−C stretching in the region 700−950 cm^{-1}, signals related to C−C, C−O stretching, and the C−O−H bending in the region 950−1200 cm^{-1} as well as a broad band between 3000 and 3600 cm^{-1} due to the stretching of O−H groups. The bands between 2800 and 3000 cm^{-1} are characteristic of C−H stretching and the signal at 1642 cm^{-1} was attributed to the bending of the absorbed water.[43] In the spectra of plasticized starch films (Figure 4b−f), in addition to the typical starch bands, some characteristic signals of the corresponding added IL can be observed (Figure S4). It is important to note that the film spectra showed no signals of additional bands, indicating that the ionic liquids did not react with the starch. However, in the region 3200−3400 cm^{-1}, slight changes in the position of the vibrational bands associated with stretching of the OH groups occurred, resulting from an interaction between the starch, the corresponding added IL, and the water molecules absorbed by the films. Indeed, when the OH groups of starch are involved in hydrogen bonding, the vibrational absorption band shifts toward lower wavenumbers. Conversely, when the hydrogen bond strength decreases, the signals shift toward higher wavenumbers. According to this effect, the interaction between monocationic ionic liquids EMIm-X and the starch chains in plasticized films depends on the anion characteristics. When $[N(CN)_2]^-$ and $[SO_4Et]^-$ anions were employed, significant shifts at higher wavenumbers were observed, from 3327 to 3340 and 3356 cm^{-1}, respectively. This suggested that these ionic liquids could weaken the hydrogen bonds between the starch chains. Using EMIm-Cl, the slight increase in wavenumbers (3330 cm^{-1}) evidenced that the chloride also weakened the hydrogen bonds between the starch chains, as reported in the literature.[21] This effect was probably not pronounced because of the opposite effect exerted by absorbed water. On the contrary, with the OAc anion, a shift toward lower wavenumbers (3279 cm^{-1}) occurred. This can be associated with an increase of hydrogen bonds related to the interaction between the OAc anions and the OH groups of starch and the concomitant greater amount of water absorbed by the films with this IL. Finally, when the imidazolium monocation was replaced with the dication structure, keeping the chloride as an anion, a reduction in the absorption wavenumber of the OH bonds (3310 cm^{-1}) took place (Figure 4f). This behavior probably reflected a stronger interaction of the dicationic IL with the OH groups of the starch chains compared to the monocationic one.[44] The other typical signals of starch in the films did not show significant shifts (Table S1).

3.5. Thermogravimetric Analysis (TGA). The thermal stability of TPS films was evaluated by using thermogravimetric analysis. Figure 5 shows the thermograms of the different starch films in comparison to that of native starch. For all of the samples, a first weight loss was observed between 25 and 150 °C, associated with the evaporation of the absorbed water. The weight loss of the native starch was about 10 wt %, which is approximately the moisture content of arrowroot starch,[28] while the water loss of the films plasticized with the ILs confirms the MC values reported in Table 1. Afterward, the films maintained the mass almost unchanged up to 230 °C. All of the plasticized films showed a very similar thermal decomposition profile. However, the thermal degradation temperature occurred between 260 and 300 °C, earlier compared to the native starch. This behavior is in agreement with results reported in the literature for films plasticized with ionic liquids.[32]

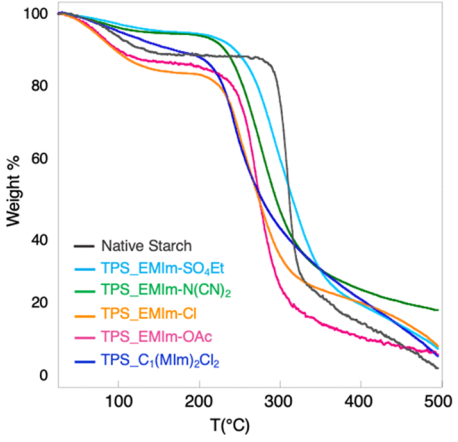

Sample	T_{deg} (°C)
Native starch	310
TPS_EMIm-SO_4Et	300
TPS_EMIm-OAc	269
TPS_EMIM-$N(CN)_2$	280
TPS_EMIm-Cl	261
TPS_ $C_1(Mim)_2Cl_2$	260

Figure 5. Thermogravimetric curves of TPS samples.

https://doi.org/10.1021/acsapm.3c01235
ACS Appl. Polym. Mater. 2023, 5, 8859−8868

The thermal stability of starch films plasticized with ionic liquids depends mainly on the nature of the anion and little on the cation.[45] In fact, the decomposition temperatures of TPS_EMIm-Cl and TPS_$C_1(Mim)_2$ Cl_2 films are quite similar. The starch film prepared by choosing $[SO_4Et]^-$ as the anion exhibited a higher thermal decomposition temperature due to the poorly coordinating nature of the anion.[46] On the other hand, the films containing chloride as the anion showed low thermal stability because of the strong coordinating effect of $[Cl]^-$.[47] A higher residual weight was observed when the anion was $[N(CN)_2]^-$, which can polymerize when heated giving solid residues.[48]

3.6. Differential Scanning Calorimetry (DSC). The glass transition temperatures were obtained from DSC analysis and evaluated as the midpoint of the heat capacity increase. In the first heating experiment performed on sealed capsules, the wet samples did not show any transition, confirming a behavior previously reported in the literature.[49] In the second series of temperature ramps, carried out on open capsules to minimize the water influence, the thermograms of the dry samples showed a transition (referred to as dry T_g) whose values are reported in Table 2.

Table 2. Glass Transition Temperatures of the Different Dry TPS Film

sample	dry T_g (°C)	ΔC_p (J gK^{-1})
starch control	120	0.259
TPS_EMIm-SO_4Et	51	0.244
TPS_EMIm-OAc	78	0.343
TPS_EMIm-$N(CN)_2$	55	0.263
TPS_EMIm-Cl	63	0.295
TPS_$C_1(MIm)_2$ Cl_2	104	0.525

Generally, good plasticizers should decrease the intermolecular forces between the polymer matrix and reduce the dry T_g.[43] All of the ILs used exhibited a plasticizing effect; in fact, the T_g values of the films were lower than those of native starch. An assessment of the effect of different anions for monocationic ILs showed that the lower glass transition temperatures belong to the TPS films plasticized with the $[SO_4Et]^-$ (dry T_g = 51 °C) and $[N(CN)_2]^-$ (dry T_g = 55 °C) anions, which allow greater molecular mobility of starch chains in the dry state. The evidence of this effect on the weakening of hydrogen bonds between the polymer chains had already been provided by the FTIR analysis. Instead, the higher hydrophilicity shown by the $[OAc]^-$- and $[Cl]^-$-containing samples, together with the related higher moisture content, affects their glass transition temperatures. In fact, the higher water content leads to an increase in the free volume between starch chains, occupied by water molecules.[50] When the samples are dried, the polymer structure is rearranged, forming interactions between the polymer chains, resulting in lower molecular mobility in the dry state.[51] This could be the reason for the dry T_g values of the films obtained with EMIm-Cl and EMIm-OAc being slightly higher than those of the films containing EMIm-SO_4Et and EMIm-$N(CN)_2$ as plasticizers. When dicationic ionic liquid ($C_1(Mim)_2$ Cl_2) was added to the starch, a reduction in dry T_g was still observed compared with pure starch, so that the dicationic structure also had a plasticizing effect. However, the dry T_g value (104 °C) of the film was higher than those (51−78 °C) of the films with monocationic ionic liquids. This behavior is in agreement with FTIR analysis and with the results reported in the literature on the entanglement of polymers with dicationic structure.[44] In fact, the imidazolium double ring is supposed to establish more interactions than a single ring with the starch chains, making them less mobile.

3.7. Mechanical Properties. Mechanical properties can be affected by different factors like the type and concentration of plasticizer, the starch granule remains in the matrix and the film crystallinity.[52] External factors such as the temperature, the relative humidity, and the moisture content of the samples can also assume a relevant role. Indeed, water molecules act as plasticizers too, behaving as mobility enhancers due to their low molecular weight.[53,54] Selected stress−strain curves are listed in the Supporting Information (Figure S5), while the results obtained by the mechanical tests are reported in Table 3. Due to the brittleness of the native starch film, it was not possible to perform tensile tests, while the results obtained for the TPS samples confirmed the plasticizing effect of all the ILs. Young's modulus (E), which measures the stiffness of the materials at low deformation, ranged from 14 to 1600 MPa, the tensile strength (TS) from 1 to 29 MPa, and the elongation at break (ε%) from 4 to 42%.

Table 3. Young's Modulus (E), Tensile Strength (TS), and Elongation at Break (ε%) of the TPS Films

sample	Young modulus (E) (Mpa)	tensile strength (TS) (MPa)	elongation at break (ε) (%)
native starch	-	-	-
TPS_EMIm-SO_4Et	70 ± 8	6 ± 1	35 ± 4
TPS_EMIm-OAc	53 ± 8	3 ± 1	42 ± 4
TPS_EMIm-$N(CN)_2$	45 ± 4	3 ± 1	40 ± 3
TPS_EMIm-Cl	14 ± 1	1 ± 1	22 ± 1
TPS_$C_1(Mim)_2$ Cl_2	1600 ± 400	29 ± 5	4 ± 1

Films with monocationic ILs with different anions showed comparable mechanical properties. A slight difference was found for the film obtained using EMIm-Cl as an additive, which exhibited lower Young's modulus and tensile strength values, appearing more compliant. Probably this is due to the ability of the chloride ion to weaken the interactions between the starch chains as shown by FTIR analysis, and the higher water content of films with EMIm-Cl compared with those containing EMIm-$N(CN)_2$ and EMIm-SO_4Et.

For TPS_$C_1(Mim)_2Cl_2$, the higher steric hindrance of the dication structure favored the macromolecular entanglements of the starch matrix, leading to a very stiff material with a Young Modulus of 1600 MPa, a tensile strength of 29 MPa, and a very low ε% of 4%.

3.8. Electrochemical Properties. Using ILs as plasticizers of starch, the resulting films can obtain interesting features that are related to electrical conductivity, making these materials good candidates as constituents in many applications of flexible electronics.[22] Conductivity is greatly dependent on the ion diffusivity and mobility favored by small size and delocalized charge[55] as well as by a polymer matrix that facilitates their movement. The conductance of the TPS film can also be affected by the absorbed water.[56] The results of the impedance measurements on all prepared films after conditioning at a relative humidity of 50% at room temperature are shown in Table 4. All EMIm-X films showed higher conductivity than that of $C_1(MIm)_2Cl_2$. In fact, the dication interactions with the polymer chains brought about a decrease in mobility and,

https://doi.org/10.1021/acsapm.3c01235
ACS Appl. Polym. Mater. 2023, 5, 8859−8868

Table 4. Ionic Conductivity of TPS Films at RT and 50 wt % RH and the Electrochemical Stability Windows

sample	σ (S cm^{-1})	working electrochemical window
TPS_EMIm-SO_4Et	6.3×10^{-7}	2.4 V
TPS_EMIm-OAc	3.6×10^{-6}	2.4 V
TPS_EMIm-$N(CN)_2$	1.4×10^{-5}	2.0 V
TPS_EMIm-Cl	2.7×10^{-5}	1.2 V
TPS_$C_1(MIm)_2$ Cl_2	9.1×10^{-8}	1.8 V

consequently, a significant reduction in ionic conductivity. Among TPS_EMIm-X, the highest conductivity value belongs to TPS_EMIm-Cl. This could be caused by the small chloride size and the good flexibility of the material, evidenced by Young's modulus value and higher moisture content (Table 1).

The electrochemical stability of conducting polymers in contact with electrode materials is a key issue to ensure adequate performance in their applications as solid electrolytes in batteries since secondary and decomposition reactions must be avoided. Knowledge of the electrochemical stability window is one of the main aspects required for the applications of films.[23] The working electrochemical window for all of the TPS films was determined by linear sweep voltammetry measurements. The current vs voltage plots for all of the samples are shown in Figure S6, while the calculated electrochemical stability window values for the TPS films are listed in Table 4.

Although TPS_EMIm-Cl showed the highest conductive capacity, its stability window is between 0 and about 1.2 V, narrower than that of the other prepared films. However, it is worth noting that this value is still adequate for use in proton batteries, for which the required standard value is ~1 V.[57]

The temperature dependence of ionic conductivity was evaluated for films plasticized with monocationic ILs, which showed better conductivity (Figure 6). The measurements were carried out on a temperature scan from 18 up to 70 °C, at two values of relative humidity (RH = 40% and RH = 50%), to investigate the effect of conditioning.

The conductivity of all of the samples increased as the temperature increased with no abrupt change, indicating no phase transition in the explored temperature range.[58] Moreover, the regression values of the temperature-dependence fit were close to unity, implying that all of the samples follow the Arrhenius law (eq 4)

$$\sigma = Ae^{-E_a/kT} \tag{4}$$

where A is a constant, E_a is the activation energy, k is the Boltzmann constant, and T is the absolute temperature.

Based on these results, the ions constituting the IL dissociate in the starch matrix and an ion hopping mechanism within the polymer matrix is inferred.[59,60]

The conductivity of TPS_EMIm-SO_4Et, TPS_EMIm-N-$(CN)_2$, and TPS_EMIm-Cl films conditioned at RH of 40% decreased and the activation energy increased with respect to the results acquired at RH = 50% (Table S2). On the other hand, an interesting result was found for films plasticized with EMIm-OAc, for which it was observed that the conductivity and the activation energy at 50 and 40% RH remained almost unchanged. This behavior is probably due to the ability of the acetate anion to form stronger hydrogen bonds with respect to the other anions[61] so that the amount of water in the film remained unchanged at 40% humidity. This suggests greater stability of the EMIm-OAc plasticized film compared to the others in the relative humidity range of 40−50%.

4. CONCLUSIONS

In this work, starch films plasticized with imidazolium-based ionic liquids were prepared by a solution casting method. The effect of different anions (namely, $[SO_4Et]^-$, $[N(CN)_2]^-$, $[OAc]^-$, and $[Cl]^-$) and the monocationic/dicationic structure on the characteristics of the resulting films was evaluated.

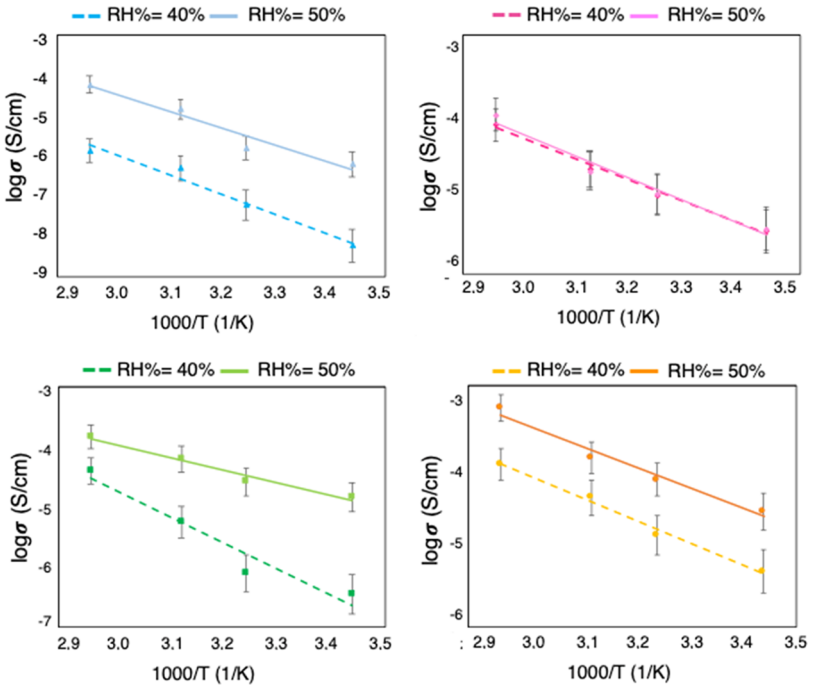

Figure 6. Variation of ionic conductivity with temperature at RH = 40% and RH = 50%.

https://doi.org/10.1021/acsapm.3c01235
ACS Appl. Polym. Mater. 2023, 5, 8859−8868

All of the prepared films had a homogeneous appearance and were transparent. The results by DSC, XRD, and FTIR analyses and mechanical tests confirmed that all of the considered ILs had a plasticizing effect. A decrease in dry T_g values compared with that of native starch was observed by DSC for all films. XRD spectra showed a reduction in film crystallinity compared to starch alone. In addition, interactions between the IL molecules and starch chains were observed for all samples analyzed by FTIR. Stress−strain experiments showed that the addition of the IL brought about a substantial increase in the toughness of the otherwise very brittle starch. However, the different anions and the replacement of the monocationic structure with a dicationic structure led to the production of films with different characteristics.

The anions $[N(CN)_2]^-$ or $[SO_4Et]^-$ caused a lower water content in the final films than those using $[Cl]^-$ and $[OAc]^-$. Regarding thermal resistance, the film obtained with EMIm-SO_4Et showed the highest degradation temperature. Films with EMIm-OAc, EMIm-Cl displayed a prevalent B-type structure compared to V_H-type after recrystallization, which may be associated with a greater hydration of the films. Moreover, FTIR analysis pointed out a structure-dependent interaction between the starch chains and ILs. In TPS_EMIm-SO_4Et, TPS_EMIm-$N(CN)_2$, and TPS_EMIm-Cl, a reduction of hydrogen bonds between the starch chains was observed. Instead, when $[OAc]^-$ was chosen as the anion, an increase in the interactions with the OH groups of starch was noticed, probably enhanced by the higher water content of this film. Mechanical testing identified the EMIm-Cl-based film as the most compliant.

By replacing the monocationic structure with a dicationic one, the plasticizing effect was reduced. The corresponding films showed a higher degree of crystallinity, a higher dry T_g, and much higher Young's modulus and tensile strength values than films with a monocationic structure. These results probably arose from increased entanglement of the starch chains with the dicationic structure, as also indicated by FTIR analysis.

All films showed good conductivity and an adequate electrochemical stability window, useful for applications as solid electrolytes. The best results in conductivity were obtained with the chloride anion, probably because of its small size and the high water content retained by the film. However, moving from EMIm-Cl to the corresponding dicationic structure, a marked reduction in conductivity was observed, confirming that the cationic portion strongly interacts with the polymer chains, making them less mobile. The ionic conductivity of the films increased with temperature, following the Arrhenius behavior. Interestingly, the conductivity of the films plasticized with EMIm-OAc was unaffected by relative humidity in the range of 40−50% RH.

These results evidenced that both anionic and cationic portions of the 1-ethyl-3-methyl imidazolium-based plasticizer have a great influence on starch-based films. The proposed multi-technique approach allowed one to gain knowledge about the different aspects of features of films, useful for selecting the appropriate ionic liquid to prepare starch base materials with the desired properties.

■ ASSOCIATED CONTENT

Supporting Information

The Supporting Information is available free of charge at https://pubs.acs.org/doi/10.1021/acsapm.3c01235.

^{1}H NMR and ^{13}C NMR spectra of 3,3′-methylenbis(1-methyl-1*H*-imidazol-3-ium) dichloride; images of the appearance of the films; FTIR spectra of the used ionic liquids; FTIR absorption bands of all prepared films; stress−strain curves of the prepared TPS films; plot of working electrochemical windows for all of the TPS films; Ionic conductivity of TPS films at RH = 40%; and activation energy of TPS films at RH = 40% and RH = 50% (PDF)

■ AUTHOR INFORMATION

Corresponding Author

Monica Orsini − *Department of Industrial, Electronic and Mechanical Engineering, Roma Tre University, 00146 Rome, Italy;* orcid.org/0000-0003-0767-5353; Email: monica.orsini@uniroma3.it

Authors

Susanna Romano − *Department of Industrial, Electronic and Mechanical Engineering, Roma Tre University, 00146 Rome, Italy;* orcid.org/0000-0001-8343-0257

Serena De Santis − *Department of Industrial, Electronic and Mechanical Engineering, Roma Tre University, 00146 Rome, Italy*

Andrea Martinelli − *Department of Chemistry, University of Rome "La Sapienza", 00185 Rome, Italy;* orcid.org/0000-0002-6401-9988

Lorenzo Augusto Rocchi − *Department of Chemistry, University of Rome "La Sapienza", 00185 Rome, Italy;* orcid.org/0000-0002-2565-5324

Daniele Rocco − *Department of Basic and Applied Sciences for Engineering, University of Rome "La Sapienza", Rome 00161, Italy*

Giovanni Sotgiu − *Department of Industrial, Electronic and Mechanical Engineering, Roma Tre University, 00146 Rome, Italy*

Complete contact information is available at: https://pubs.acs.org/10.1021/acsapm.3c01235

Notes

The authors declare no competing financial interest.

■ REFERENCES

(1) Porta, R.; Sabbah, M.; Di Pierro, P. Biopolymers as Food Packaging Materials. *Int. J. Mol. Sci.* **2020**, *21* (14), 4942.

(2) Porta, R. The Plastics Sunset and the Bio-Plastics Sunrise. *Coatings* **2019**, *9* (8), 526.

(3) Agarwal, S. Major Factors Affecting the Characteristics of Starch Based Biopolymer Films. *Eur. Polym. J.* **2021**, *160*, No. 110788.

(4) Chivrac, F.; Angellier-Coussy, H.; Guillard, V.; Pollet, E.; Avérous, L. How Does Water Diffuse in Starch/Montmorillonite Nano-Biocomposite Materials? *Carbohydr. Polym.* **2010**, *82* (1), 128−135.

(5) Souza, A. C.; Benze, R.; Ferrão, E. S.; Ditchfield, C.; Coelho, A. C. V.; Tadini, C. C. Cassava Starch Biodegradable Films: Influence of Glycerol and Clay Nanoparticles Content on Tensile and Barrier Properties and Glass Transition Temperature. *LWT* **2012**, *46* (1), 110−117.

(6) Avérous, L. Biodegradable Multiphase Systems Based on Plasticized Starch: A Review. *J. Macromol. Sci., Polym. Rev.* **2004**, *44* (3), 231−274.

(7) Jenkins, P. J.; Donald, A. M. The Influence of Amylose on Starch Granule Structure. *Int. J. Biol. Macromol.* **1995**, *17* (6), 315−321.

(8) Wang, W.; Wang, H.; Jin, X.; Wang, H.; Lin, T.; Zhu, Z. Effects of Hydrogen Bonding on Starch Granule Dissolution, Spinnability of Starch Solution, and Properties of Electrospun Starch Fibers. *Polymer (Guildf)* **2018**, *153*, 643−652.
(9) Shah, U.; Naqash, F.; Gani, A.; Masoodi, F. A. Art and Science behind Modified Starch Edible Films and Coatings: A Review. *Compr Rev. Food Sci. Food Saf* **2016**, *15* (3), 568−580.
(10) Laohakunjit, N.; Noomhorm, A. Effect of Plasticizers on Mechanical and Barrier Properties of Rice Starch Film. *Starch/Staerke* **2004**, *56* (8), 348−356.
(11) Masina, N.; Choonara, Y. E.; Kumar, P.; du Toit, L. C.; Govender, M.; Indermun, S.; Pillay, V. A Review of the Chemical Modification Techniques of Starch. *Carbohydr. Polym.* **2017**, *157*, 1226−1236.
(12) Weng, T.; He, Z.; Zhang, Z.; Chen, Y.; Zhou, M.; Wen, B. A Facile Method of Functional Derivatization Based on Starch Acetoacetate. *Carbohydr. Polym.* **2022**, *289*, No. 119468.
(13) Vieira, M. G. A.; da Silva, M. A.; dos Santos, L. O.; Beppu, M. M. Natural-Based Plasticizers and Biopolymer Films: A Review. *Eur. Polym. J.* **2011**, *47* (3), 254−263.
(14) Galdeano, M. C.; Mali, S.; Grossmann, M. V. E.; Yamashita, F.; García, M. A. Effects of Plasticizers on the Properties of Oat Starch Films. *Mater. Sci. Eng.: C* **2009**, *29* (2), 532−538.
(15) Niazi, M. B. K.; Zijlstra, M.; Broekhuis, A. A. Influence of Plasticizer with Different Functional Groups on Thermoplastic Starch. *J. Appl. Polym. Sci.* **2015**, *132* (22), n/a.
(16) Wang, J.; Cheng, F.; Zhu, P. Structure and Properties of Urea-Plasticized Starch Films with Different Urea Contents. *Carbohydr. Polym.* **2014**, *101*, 1109−1115.
(17) Shi, R.; Zhang, Z.; Liu, Q.; Han, Y.; Zhang, L.; Chen, D.; Tian, W. Characterization of Citric Acid/Glycerol Co-Plasticized Thermoplastic Starch Prepared by Melt Blending. *Carbohydr. Polym.* **2007**, *69* (4), 748−755.
(18) Tyagi, V.; Bhattacharya, B. Role of Plasticizers in Bioplastics. *MOJ Food Process. Technol.* **2019**, *7* (4), 128−130, DOI: 10.15406/mojfpt.2019.07.00231.
(19) Rocco, D.; Folgueiras-Amador, A. A.; Brown, R. C. D.; Feroci, M. First Example of Organocatalysis by Cathodic N-Heterocyclic Carbene Generation and Accumulation Using a Divided Electrochemical Flow Cell. *Beilstein J. Org. Chem.* **2022**, *18*, 979−990.
(20) Ren, F.; Wang, J.; Xie, F.; Zan, K.; Wang, S.; Wang, S. Applications of Ionic Liquids in Starch Chemistry: A Review. *Green Chem.* **2020**, *22* (7), 2162−2183.
(21) Sankri, A.; Arhaliass, A.; Dez, I.; Gaumont, A. C.; Grohens, Y.; Lourdin, D.; Pillin, I.; Rolland-Sabaté, A.; Leroy, E. Thermoplastic Starch Plasticized by an Ionic Liquid. *Carbohydr. Polym.* **2010**, *82* (2), 256−263.
(22) Xiang, H.; Li, Z.; Liu, H.; Chen, T.; Zhou, H.; Huang, W. Green Flexible Electronics Based on Starch. *npj Flexible Electron.* **2022**, *6* (1), 15.
(23) Zhao, Y.; Wang, L.; Zhou, Y.; Liang, Z.; Tavajohi, N.; Li, B.; Li, T. Solid Polymer Electrolytes with High Conductivity and Transference Number of Li Ions for Li-Based Rechargeable Batteries. *Adv. Sci.* **2021**, *8* (7), No. 2003675.
(24) Rocco, D.; Chiarotto, I.; D'Anna, F.; Mattiello, L.; Pandolfi, F.; Rizzo, C.; Feroci, M. Cathodic Behaviour of Dicationic Imidazolium Bromides: The Role of the Spacer. *ChemElectroChem* **2019**, *6* (16), 4275−4283.
(25) Hooshyari, K.; Javanbakht, M.; Adibi, M. Novel Composite Membranes Based on PBI and Dicationic Ionic Liquids for High Temperature Polymer Electrolyte Membrane Fuel Cells. *Electrochim. Acta* **2016**, *205*, 142−152.
(26) Khan, A. S.; Man, Z.; Arvina, A.; Bustam, M. A.; Nasrullah, A.; Ullah, Z.; Sarwono, A.; Muhammad, N. Dicationic Imidazolium Based Ionic Liquids: Synthesis and Properties. *J. Mol. Liq.* **2017**, *227*, 98−105.
(27) Pandolfi, F.; Bortolami, M.; Feroci, M.; Fornari, A.; Scarano, V.; Rocco, D. Recent Advances in Imidazolium-Based Dicationic Ionic Liquids as Organocatalysts: A Mini-Review. *Materials* **2022**, *15* (3), 866.
(28) Nogueira, G. F.; Fakhouri, F. M.; de Oliveira, R. A. Extraction and Characterization of Arrowroot (Maranta Arundinaceae L.) Starch and Its Application in Edible Films. *Carbohydr. Polym.* **2018**, *186*, 64−72.
(29) Penn, K. R.; Anders, E. J.; Lindsay, V. N. G. Expedient Synthesis of Bis(Imidazolium) Dichloride Salts and Bis(NHC) Complexes from Imidazoles Using DMSO as a Key Polar Additive. *Organometallics* **2021**, *40* (23), 3871−3875.
(30) Thakur, R.; Pristijono, P.; Scarlett, C. J.; Bowyer, M.; Singh, S. P.; Vuong, Q. V. Starch-Based Films: Major Factors Affecting Their Properties. *Int. J. Biol. Macromol.* **2019**, *132*, 1079−1089.
(31) Ben Slima, S.; Trabelsi, I.; Ktari, N.; Bardaa, S.; Elkaroui, K.; Bouaziz, M.; Abdeslam, A.; Ben Salah, R. Novel *Sorghum bicolor* (L.) Seed Polysaccharide Structure, Hemolytic and Antioxidant Activities, and Laser Burn Wound Healing Effect. *Int. J. Biol. Macromol.* **2019**, *132*, 87−96.
(32) Xie, F.; Flanagan, B. M.; Li, M.; Sangwan, P.; Truss, R. W.; Halley, P. J.; Strounina, E.; Whittaker, A. K.; Gidley, M. J.; Dean, K. M.; Shamshina, J. L.; Rogers, R. D.; McNally, T. Characteristics of Starch-Based Films Plasticised by Glycerol and by the Ionic Liquid 1-Ethyl-3-Methylimidazolium Acetate: A Comparative Study. *Carbohydr. Polym.* **2014**, *111*, 841−848.
(33) Tarique, J.; Sapuan, S. M.; Khalina, A. Effect of Glycerol Plasticizer Loading on the Physical, Mechanical, Thermal, and Barrier Properties of Arrowroot (Maranta Arundinacea) Starch Biopolymers. *Sci. Rep.* **2021**, *11* (1), No. 13900, DOI: 10.1038/s41598-021-93094-y.
(34) Abera, G.; Woldeyes, B.; Demash, H. D.; Miyake, G. The Effect of Plasticizers on Thermoplastic Starch Films Developed from the Indigenous Ethiopian Tuber Crop Anchote (Coccinia Abyssinica) Starch. *Int. J. Biol. Macromol.* **2020**, *155*, 581−587.
(35) Basiak, E.; Lenart, A.; Debeaufort, F. Effect of Starch Type on the Physico-Chemical Properties of Edible Films. *Int. J. Biol. Macromol.* **2017**, *98*, 348−356.
(36) Nordin, N.; Othman, S. H.; Rashid, S. A.; Basha, R. K. Effects of Glycerol and Thymol on Physical, Mechanical, and Thermal Properties of Corn Starch Films. *Food Hydrocolloids* **2020**, *106*, No. 105884, DOI: 10.1016/j.foodhyd.2020.105884.
(37) Ghasemlou, M.; Aliheidari, N.; Fahmi, R.; Shojaee-Aliabadi, S.; Keshavarz, B.; Cran, M. J.; Khaksar, R. Physical, Mechanical and Barrier Properties of Corn Starch Films Incorporated with Plant Essential Oils. *Carbohydr. Polym.* **2013**, *98* (1), 1117−1126.
(38) Lai, W. F.; Wong, W. T. Edible Clusteroluminogenic Films Obtained from Starch of Different Botanical Origins for Food Packaging and Quality Management of Frozen Foods. *Membranes* **2022**, *12* (4), No. 437, DOI: 10.3390/membranes12040437.
(39) Cheetham, N. W. H.; Tao, L. Variation in Crystalline Type with Amylose Content in Maize Starch Granules: An X-Ray Powder Diffraction Study. *Carbohydr. Polym.* **1998**, *36* (4), 277−284.
(40) Pérez, S.; Bertoft, E. The Molecular Structures of Starch Components and Their Contribution to the Architecture of Starch Granules: A Comprehensive Review. *Starch/Staerke* **2010**, *62* (8), 389−420.
(41) Zhang, Y.; Rempel, C. Retrogradation and Antiplasticization of Thermoplastic Starch. In *Thermoplastic Elastomers*; InTech, 2012 DOI: 10.5772/35848.
(42) Kong, L.; Lee, C.; Kim, S. H.; Ziegler, G. R. Characterization of Starch Polymorphic Structures Using Vibrational Sum Frequency Generation Spectroscopy. *J. Phys. Chem. B* **2014**, *118* (7), 1775−1783.
(43) Valderrama Solano, A. C.; Rojas de Gante, C. Development of Biodegradable Films Based on Blue Corn Flour with Potential Applications in Food Packaging. Effects of Plasticizers on Mechanical, Thermal, and Microstructural Properties of Flour Films. *J. Cereal Sci.* **2014**, *60* (1), 60−66.
(44) He, X.; Kong, M.; Niu, Y.; Li, G. Entanglement and Relaxation of Poly(Methyl Methacrylate) Chains in Imidazolium-Based Ionic

Liquids with Different Cationic Structures. *Macromolecules* **2020**, *53* (18), 7865−7875.
(45) Huang, Y.; Chen, Z.; Crosthwaite, J. M.; NVK Aki, S.; Brennecke, J. F. Thermal Stability of Ionic Liquids in Nitrogen and Air Environments. *J. Chem. Thermodyn.* **2021**, *161*, No. 106560.
(46) Crosthwaite, J. M.; Muldoon, M. J.; Dixon, J. K.; Anderson, J. L.; Brennecke, J. F. Phase Transition and Decomposition Temperatures, Heat Capacities and Viscosities of Pyridinium Ionic Liquids. *J. Chem. Thermodyn.* **2005**, *37* (6), 559−568.
(47) Ngo, H. L.; LeCompte, K.; Hargens, L.; McEwen, A. B. Thermal Properties of Imidazolium Ionic Liquids. *Thermochim. Acta* **2000**, *357*−*358*, 97−102.
(48) Chambreau, S. D.; Schenk, A. C.; Sheppard, A. J.; Yandek, G. R.; Vaghjiani, G. L.; Maciejewski, J.; Koh, C. J.; Golan, A.; Leone, S. R. Thermal Decomposition Mechanisms of Alkylimidazolium Ionic Liquids with Cyano-Functionalized Anions. *J. Phys. Chem. A* **2014**, *118* (47), 11119−11132.
(49) Forssell, P. Ageing of Rubbery Thermoplastic Barley and Oat Starches. *Carbohydr. Polym.* **1999**, *39* (1), 43−51.
(50) Lai, H. C.; Karim, A. A.; Chee, C. S. Effects of Water-Glycerol and Water-Sorbitol Interactions on the Physical Properties of Konjac Glucomannan Films. *J. Food Sci.* **2006**, *71* (2), E62−E67, DOI: 10.1111/j.1365-2621.2006.tb08898.x.
(51) Shogren, R. Preparation, Thermal Properties, and Extrusion of High-Amylose Starch Acetates. *Carbohydr. Polym.* **1996**, *29* (1), 57−62.
(52) Xie, F.; Flanagan, B. M.; Li, M.; Truss, R. W.; Halley, P. J.; Gidley, M. J.; McNally, T.; Shamshina, J. L.; Rogers, R. D. Characteristics of Starch-Based Films with Different Amylose Contents Plasticised by 1-Ethyl-3-Methylimidazolium Acetate. *Carbohydr. Polym.* **2015**, *122*, 160−168.
(53) Karbowiak, T.; Hervet, H.; Léger, L.; Champion, D.; Debeaufort, F.; Voilley, A. Effect of Plasticizers (Water and Glycerol) on the Diffusion of a Small Molecule in Iota-Carrageenan Biopolymer Films for Edible Coating Application. *Biomacromolecules* **2006**, *7* (6), 2011−2019.
(54) Mali, S.; Sakanaka, L. S.; Yamashita, F.; Grossmann, M. V. E. Water Sorption and Mechanical Properties of Cassava Starch Films and Their Relation to Plasticizing Effect. *Carbohydr. Polym.* **2005**, *60* (3), 283−289.
(55) Zhang, B.; Xie, F.; Shamshina, J. L.; Rogers, R. D.; McNally, T.; Wang, D. K.; Halley, P. J.; Truss, R. W.; Zhao, S.; Chen, L. Facile Preparation of Starch-Based Electroconductive Films with Ionic Liquid. *ACS Sustainable Chem. Eng.* **2017**, *5* (6), 5457−5467, DOI: 10.1021/acssuschemeng.7b00788.
(56) Ning, W.; Xingxiang, Z.; Haihui, L.; Benqiao, H. 1-Allyl-3-Methylimidazolium Chloride Plasticized-Corn Starch as Solid Biopolymer Electrolytes. *Carbohydr. Polym.* **2009**, *76* (3), 482−484.
(57) Kadir, M. F. Z.; Arof, A. K. Application of PVA-Chitosan Blend Polymer Electrolyte Membrane in Electrical Double Layer Capacitor. *Mater. Res. Innovations* **2011**, *15* (SUPPL. 2), s217−s220, DOI: 10.1179/143307511X13031890749299.
(58) Ramesh, S.; Yin, T. S.; Liew, C. W. Effect of Dibutyl Phthalate as Plasticizer on High-Molecular Weight Poly(Vinyl Chloride)-Lithium Tetraborate-Based Solid Polymer Electrolytes. *Ionics (Kiel)* **2011**, *17* (8), 705−713.
(59) Liew, C. W.; Ramesh, S.; Ramesh, K.; Arof, A. K. Preparation and Characterization of Lithium Ion Conducting Ionic Liquid-Based Biodegradable Corn Starch Polymer Electrolytes. *J. Solid State Electrochem.* **2012**, *16* (5), 1869−1875.
(60) Muthukrishnan, M.; Shanthi, C.; Selvasekarapandian, S.; Premkumar, R. Biodegradable Flexible Proton Conducting Solid Biopolymer Membranes Based on Pectin and Ammonium Salt for Electrochemical Applications. *Int. J. Hydrogen Energy* **2023**, *48* (14), 5387−5401.
(61) Pike, S. J.; Hutchinson, J. J.; Hunter, C. A. H-Bond Acceptor Parameters for Anions. *J. Am. Chem. Soc.* **2017**, *139* (19), 6700−6706.

https://doi.org/10.1021/acsapm.3c01235
ACS Appl. Polym. Mater. 2023, 5, 8859−8868